

Technical Notes

TECHNICAL NOTES are short manuscripts describing new developments or important results of a preliminary nature. These Notes should not exceed 2500 words (where a figure or table counts as 200 words). Following informal review by the Editors, they may be published within a few months of the date of receipt. Style requirements are the same as for regular contributions (see inside back cover).

Vertically Reinforced 1-3 Piezoelectric Composites for Active Damping of Functionally Graded Plates

M. C. Ray* and R. C. Batra†

Virginia Polytechnic Institute and State University,
Blacksburg, Virginia 24061

DOI: 10.2514/1.26183

Introduction

MONOLITHIC piezoelectric materials (PZTs) have been widely used as distributed sensors and actuators for developing smart structures with self-monitoring and self-controlling capabilities [1–10]. However, their major drawback is low control authority as the magnitude of their electromechanical coefficients is very small. The situation can be improved by using an active constrained layer damping (ACLAD) treatment [11,12] which consists of a layer of a viscoelastic material constrained between a host structure and an active constraining PZT layer. When the constraining layer is activated with a voltage applied to the PZT layer, the shearing deformations of the viscoelastic layer are enhanced to improve the damping characteristics of the overall structures. Since its inception, the ACLAD treatment has been extensively used for efficient and reliable control of flexible structures [13–17].

Piezoelectric composites, also called piezocomposites, have emerged as a new class of smart materials and have found wide applications as distributed actuators and sensors. A piezocomposite, composed of PZT reinforcements embedded in a conventional epoxy matrix, provides a wide range of effective material properties not offered by existing PZTs, is anisotropic, and has good conformability and strength. We note that laminae of vertically reinforced 1-3 piezocomposites are commercially available [18] and are being effectively used as underwater high-frequency transducers and in medical imaging applications [19,20]. A 1-3 piezocomposite lamina has PZT fibers vertically reinforced in the epoxy matrix across the thickness of the lamina, the fibers are poled along their length, and the top and the bottom surfaces of the lamina are electroded. The effective PZT coefficient (e_{33}) of the 1-3 piezocomposite, which equals the normal stress (σ_z) along the fiber direction due to a unit electric field applied across the thickness of the piezocomposite lamina, is much larger than the effective coefficients e_{31} and e_{32} which signify the induced normal stresses (σ_x , σ_y) in directions transverse to the fiber. However, very little attention has been paid to

using these 1-3 piezocomposites for active vibration control [21]. Until recently, the host structure in a smart system has been considered to be made of a homogeneous and either isotropic or orthotropic material. Recently, functionally graded materials (FGMs) which exhibit smooth variation of material properties in one or more directions have been investigated for developing high-performance smart FG structures [22–27]. We also note that Batra and Geng [12] considered a FG viscoelastic layer but a homogeneous PZT constraining layer and performed the three-dimensional transient analysis of the problem with the finite element method (FEM). However, it appears that the performance of a vertically reinforced 1-3 piezocomposite has not yet been investigated for active control of FG structures.

Here, we use a first-order shear deformation plate theory (FSDT) and the FEM to analyze ACLD of FG plates with the objective of investigating the performance of the vertically reinforced 1-3 piezocomposite as the material of the constraining layer.

Problem Statement and Basic Equations

A schematic sketch of the problem studied is shown in Fig. 1. The thicknesses of the substrate FG plate, piezocomposite layer, and the viscoelastic layer are denoted by h , h_p , and h_v , respectively. The midsurface of the substrate plate is taken as the reference plane with the origin of the rectangular Cartesian coordinate system (xyz) located in it such that lines $x = 0$, a and $y = 0$, b represent boundaries of the substrate plate.

The overall smart structure is assumed to be thin; thus the FSDT is used to model its deformations. Accordingly, displacements u , v , and w of a point along the x , y , and z directions, respectively, are expressed as

$$u(x, y, z, t) = u_0(x, y, t) + \lambda_1(z)\theta_x(x, y, t) + \lambda_2(z)\phi_x(x, y, t) + \lambda_3(z)\gamma_x(x, y, t) \quad (1)$$

$$v(x, y, z, t) = v_0(x, y, t) + \lambda_1(z)\theta_y(x, y, t) + \lambda_2(z)\phi_y(x, y, t) + \lambda_3(z)\gamma_y(x, y, t) \quad (2)$$

$$w(x, y, z, t) = w_0(x, y, t) + \lambda_1(z)\theta_z(x, y, t) + \lambda_2(z)\phi_z(x, y, t) + \lambda_3(z)\gamma_z(x, y, t) \quad (3)$$

where $\lambda_1(z) = z - \langle z - h_2 \rangle$, $\lambda_2(z) = \langle z - h_2 \rangle - \langle z - h_3 \rangle$, $\lambda_3(z) = \langle z - h_3 \rangle$, $h_2 = h/2$, and $h_3 = h/2 + h_v$. Variables u_0 , v_0 , and w_0 represent the generalized translational displacement of a point (x, y) on the reference plane ($z = 0$) along the x , y , and z directions, respectively; θ_x , ϕ_x , and γ_x denote the generalized rotations of normals to the midsurface of the substrate plate, the viscoelastic layer and the piezocomposite layer, respectively, in the xz plane while θ_y , ϕ_y , and γ_y represent their generalized rotations in the yz plane. Variables θ_z , ϕ_z , and γ_z are generalized displacements representing gradients with respect to z of the transverse displacement in the substrate plate, the viscoelastic layer, and the piezocomposite layer, respectively, t is the time variable and a function within the bracket $\langle \rangle$ represents an appropriate singularity function for satisfying the continuity of displacements at an interface between any two

Received 26 June 2006; revision received 14 February 2007; accepted for publication 11 March 2007. Copyright © 2007 by the American Institute of Aeronautics and Astronautics, Inc. All rights reserved. Copies of this paper may be made for personal or internal use, on condition that the copier pay the \$10.00 per-copy fee to the Copyright Clearance Center, Inc., 222 Rosewood Drive, Danvers, MA 01923; include the code 0001-1452/07 \$10.00 in correspondence with the CCC.

*Visiting Scholar, Department of Engineering Science and Mechanics, MC 0219.

†Professor, Department of Engineering Science and Mechanics, MC 0219.

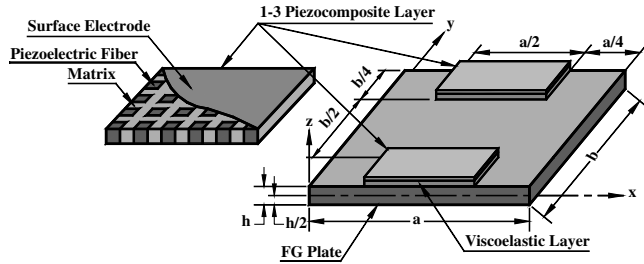


Fig. 1 Schematic sketch of a functionally graded plate integrated with patches of a viscoelastic layer and a constraining layer composed of 1-3 piezoelectric composite.

adjoining layers. Allowing for generalized rotations of normal to be different in each layer should help satisfy the continuity of tractions at these interfaces.

We assume that the FGM composed of two homogenous phases, ceramic and metal, is isotropic and linear elastic with Young's modulus (\mathbf{E}_{FG}) and mass density (ρ_{FG}) varying only in the (z) direction according to

$$\begin{aligned} \mathbf{E}_{FG}(z) &= (\mathbf{E}_c - \mathbf{E}_m) \left\{ \frac{1}{2} + (-1)^k \frac{z}{h} \right\}^n + \mathbf{E}_m \quad \text{and} \\ \rho_{FG}(z) &= (\rho_c - \rho_m) \left\{ \frac{1}{2} + (-1)^k \frac{z}{h} \right\}^n + \rho_m \end{aligned} \quad (4)$$

where \mathbf{E}_c and ρ_c are Young's modulus and Poisson's ratio of the ceramic phase, respectively, \mathbf{E}_m and ρ_m are the same for the metallic phase, n is the power law exponent, and k is a positive integer. Note that the top surface of the FG plate will be either the softest (metallic) or the stiffest (ceramic) according as k equals 1 or 2, respectively. Poisson's ratio ν of the FGM is assumed to be a constant [28] because it does not vary much for several combinations of ceramics and metals. It is also assumed that the electric field \mathbf{E}_z applied to the piezocomposite layer is along the z direction. To implement the selective integration rule for deriving the stiffness matrices of an element corresponding to bending and transverse shear deformations separately, stresses and strains at a point are grouped as

$$\begin{aligned} \{\sigma_b\} &= [\sigma_x \quad \sigma_y \quad \sigma_{xy} \quad \sigma_z]^T, \quad \{\sigma_s\} = [\sigma_{xz} \quad \sigma_{yz}]^T \\ \{\epsilon_b\} &= [\epsilon_x \quad \epsilon_y \quad \epsilon_{xy} \quad \epsilon_z]^T \quad \text{and} \quad \{\epsilon_s\} = [\epsilon_{xz} \quad \epsilon_{yz}]^T \end{aligned} \quad (5)$$

where ϵ_x , ϵ_y , and ϵ_z are normal strains along the x , y , and z directions, respectively; ϵ_{xy} is the in-plane shear strain; and ϵ_{xz} , ϵ_{yz} are transverse shear strains while σ_x , σ_y , σ_z , σ_{xy} , σ_{xz} , and σ_{yz} are corresponding stresses. Thus constitutive relations for the FGM can be expressed as

$$\{\sigma_b\} = [\mathbf{C}_b]\{\epsilon_b\} \quad \text{and} \quad \{\sigma_s\} = [\mathbf{C}_s]\{\epsilon_s\} \quad (6)$$

and the vertically reinforced 1-3 piezocomposite are given by [19]

$$\begin{aligned} \{\sigma_b\} &= [\mathbf{C}_b]\{\epsilon_b\} - \{\mathbf{e}_b\}E_z \\ \{\sigma_s\} &= [\mathbf{C}_s]\{\epsilon_s\} \quad \text{and} \quad \mathbf{D}_z = \{\mathbf{e}_b\}^T \{\epsilon_b\} \epsilon_{33} E_z \end{aligned} \quad (7)$$

where $[\mathbf{C}_b]$ and $[\mathbf{C}_s]$ are the elastic coefficient matrices, \mathbf{D}_z equals the electric displacement in the z direction, ϵ_{33} is the dielectric constant and $\{\mathbf{e}_b\} = [e_{31} \quad e_{32} \quad 0 \quad e_{33}]^T$. The viscoelastic layer is assumed to be made of an homogenous and isotropic material. Employing the complex modulus approach, its constitutive relations can also be expressed by Eq. (6) [11,13,14].

Approximate Solution by the Finite Element Method

For brevity, the generalized degrees of freedom of a point in the overall structure are grouped into the following two vectors:

$$\begin{aligned} \{\mathbf{d}_t\} &= [u_0 \quad v_0 \quad w_0]^T \quad \text{and} \\ \{\mathbf{d}_r\} &= [\theta_x \quad \theta_y \quad \theta_z \quad \phi_x \quad \phi_y \quad \phi_z \quad \gamma_x \quad \gamma_y \quad \gamma_z]^T \end{aligned} \quad (8)$$

Using strain-displacement relations and Eq. (8), the strain vectors, given by Eq. (5), at a point in a finite element can be expressed in terms of the generalized nodal displacements ($\{\mathbf{d}_t^e\}$ and $\{\mathbf{d}_r^e\}$) of the element as follows:

$$\begin{aligned} \{\epsilon_b\} &= [\mathbf{B}_{tb}]\{\mathbf{d}_t^e\} + [\mathbf{Z}_b][\mathbf{B}_{rb}]\{\mathbf{d}_r^e\} \quad \text{and} \\ \{\epsilon_s\} &= [\mathbf{B}_{ts}]\{\mathbf{d}_t^e\} + [\mathbf{Z}_s][\mathbf{B}_{rs}]\{\mathbf{d}_r^e\} \end{aligned} \quad (9)$$

where $[\mathbf{B}_{tb}] = [\mathbf{L}_{tb}][\mathbf{N}_t]$, $[\mathbf{B}_{ts}] = [\mathbf{L}_{ts}][\mathbf{N}_t]$, $[\mathbf{Z}_b] = [\mathbf{L}_1][\lambda_1(z)\mathbf{I} \quad \lambda_2(z)\mathbf{I} \quad \lambda_3(z)\mathbf{I}]$,

$$\begin{aligned} [\mathbf{L}_{tb}] &= \begin{bmatrix} \frac{\partial}{\partial x} & 0 & 0 \\ 0 & \frac{\partial}{\partial y} & 0 \\ \frac{\partial}{\partial y} & \frac{\partial}{\partial x} & 0 \\ 0 & 0 & 0 \end{bmatrix}, \quad [\mathbf{L}_{ts}] = \begin{bmatrix} 0 & 0 & \frac{\partial}{\partial x} \\ 0 & 0 & \frac{\partial}{\partial y} \end{bmatrix} \\ [\mathbf{L}_1] &= \begin{bmatrix} 1 & 0 & 0 & 0 \\ 0 & 1 & 0 & 0 \\ 0 & 0 & 1 & 0 \\ 0 & 0 & 0 & \frac{\partial}{\partial z} \end{bmatrix}, \quad [\mathbf{B}_{rb}] = [\mathbf{L}_{rb}][\mathbf{N}_r] \end{aligned}$$

$$[\mathbf{B}_{rs}] = [\mathbf{L}_{rs}][\mathbf{N}_r]$$

$$[\mathbf{Z}_s] = [\lambda_4(z)\bar{\mathbf{I}} \quad \lambda_5(z)\bar{\mathbf{I}} \quad \lambda_6(z)\bar{\mathbf{I}} \quad \lambda_1(z)\bar{\mathbf{I}} \quad \lambda_2(z)\bar{\mathbf{I}} \quad \lambda_3(z)\bar{\mathbf{I}}]$$

$$\begin{aligned} \lambda_4(z) &= 1 - \langle z - \mathbf{h}_2 \rangle^0, \quad \lambda_5(z) = \langle z - \mathbf{h}_2 \rangle^0 - \langle z - \mathbf{h}_3 \rangle^0 \\ \lambda_6(z) &= \langle z - \mathbf{h}_3 \rangle^0 \end{aligned} \quad (10)$$

Here $[\mathbf{N}_t]$ and $[\mathbf{N}_r]$ are shape function matrices for the element, $[\mathbf{L}_{rb}]$ and $[\mathbf{L}_{rs}]$ are $(12 \cdot 9)$ operator matrices, while \mathbf{I} and $\bar{\mathbf{I}}$ are $(4 \cdot 4)$ and $(2 \cdot 2)$ identity matrices, respectively. Nonzero elements of $[\mathbf{L}_{rb}]$ and $[\mathbf{L}_{rs}]$ are given by

$$\begin{aligned} \mathbf{L}_{rb}(1, 1) &= \mathbf{L}_{rb}(3, 2) = \mathbf{L}_{rb}(5, 4) = \mathbf{L}_{rb}(7, 5) = \mathbf{L}_{rb}(9, 7) \\ &= \mathbf{L}_{rb}(11, 8) = \frac{\partial}{\partial x} \end{aligned}$$

$$\begin{aligned} \mathbf{L}_{rb}(2, 2) &= \mathbf{L}_{rb}(3, 1) = \mathbf{L}_{rb}(6, 5) = \mathbf{L}_{rb}(7, 4) = \mathbf{L}_{rb}(10, 8) \\ &= \mathbf{L}_{rb}(11, 7) = \frac{\partial}{\partial y} \end{aligned}$$

$$\mathbf{L}_{rb}(4, 3) = \mathbf{L}_{rb}(8, 6) = \mathbf{L}_{rb}(12, 9) = 1$$

$$\begin{aligned} \mathbf{L}_{rs}(1, 1) &= \mathbf{L}_{rs}(2, 2) = \mathbf{L}_{rs}(3, 4) = \mathbf{L}_{rs}(4, 5) = \mathbf{L}_{rs}(5, 7) \\ &= \mathbf{L}_{rs}(6, 8) = 1 \end{aligned}$$

$$\mathbf{L}_{rs}(7, 3) = \mathbf{L}_{rs}(9, 6) = \mathbf{L}_{rs}(11, 9) = \frac{\partial}{\partial x} \quad \text{and} \quad (11)$$

$$\mathbf{L}_{rs}(8, 3) = \mathbf{L}_{rs}(10, 6) = \mathbf{L}_{rs}(12, 9) = \frac{\partial}{\partial y}$$

Employing the principle of virtual work [13] and recognizing that $\mathbf{E}_z = -\mathbf{V}/\mathbf{h}_p$ with \mathbf{V} being the voltage applied across the piezocomposite layer thickness, we derive the following open loop equations of motion for an element:

$$[\mathbf{M}^e]\{\ddot{\mathbf{d}}_t^e\} + [\mathbf{K}_{tt}^e]\{\dot{\mathbf{d}}_t^e\} + [\mathbf{K}_{tr}^e]\{\mathbf{d}_r^e\} = \{\mathbf{F}_{tp}^e\}\mathbf{V} + \{\mathbf{F}^e\} \quad (12)$$

$$[\mathbf{K}_{tr}^e]^T \{\mathbf{d}_t^e\} + [\mathbf{K}_{tr}^e] \{\mathbf{d}_r^e\} = \{\mathbf{F}_{rp}^e\} \mathbf{V} \quad (13)$$

For an element of length \mathbf{a}_e and width \mathbf{b}_e , the element mass matrix $[\mathbf{M}^e]$, stiffness matrices $[\mathbf{K}_{tt}^e]$, $[\mathbf{K}_{tr}^e]$, $[\mathbf{K}_{rr}^e]$, the electroelastic coupling vectors $\{\mathbf{F}_{tp}^e\}$, $\{\mathbf{F}_{rp}^e\}$ and the load vector $\{\mathbf{F}^e\}$ are given by

$$[\mathbf{K}_{tt}^e] = \int_{h_1}^{h_5} \int_0^{a_e} \int_0^{b_e} ([\mathbf{B}_{tb}]^T [\mathbf{C}_b] [\mathbf{B}_{tb}] + [\mathbf{B}_{ts}]^T [\mathbf{C}_s] [\mathbf{B}_{ts}]) \mathbf{d}\mathbf{x}\mathbf{z}\mathbf{d}\mathbf{y}\mathbf{d}\mathbf{z}$$

$$[\mathbf{K}_{tr}^e] = \int_{h_1}^{h_4} \int_0^{a_e} \int_0^{b_e} ([\mathbf{B}_{tb}]^T [\mathbf{C}_b] [\mathbf{Z}_b] [\mathbf{B}_{rb}] + [\mathbf{B}_{ts}]^T [\mathbf{C}_s] [\mathbf{Z}_s] [\mathbf{B}_{rs}]) \mathbf{d}\mathbf{x}\mathbf{d}\mathbf{y}\mathbf{d}\mathbf{z}$$

$$[\mathbf{K}_{rr}^e] = \int_{h_1}^{h_4} \int_0^{a_e} \int_0^{b_e} ([\mathbf{B}_{rb}]^T [\mathbf{Z}_b]^T [\mathbf{C}_b] [\mathbf{Z}_b] [\mathbf{B}_{rb}]^T + [\mathbf{B}_{rs}]^T [\mathbf{Z}_s]^T [\mathbf{C}_s] [\mathbf{Z}_s] [\mathbf{B}_{rs}]) \mathbf{d}\mathbf{x}\mathbf{d}\mathbf{y}\mathbf{d}\mathbf{z}$$

$$[\mathbf{M}^e] = \int_0^{a_e} \int_0^{b_e} \bar{\mathbf{m}} [\mathbf{N}_t]^T [\mathbf{N}_t] \mathbf{d}\mathbf{x}\mathbf{d}\mathbf{y}$$

$$\bar{\mathbf{m}} = \int_{-h/2}^{h/2} \rho_{FG} \mathbf{d}\mathbf{z} + \rho_v \mathbf{h}_v + \rho_p \mathbf{h}_p$$

$$\{\mathbf{F}^e\} = \int_0^{a_e} \int_0^{b_e} [\mathbf{N}_t]^T \{\mathbf{f}\} \mathbf{d}\mathbf{x}\mathbf{d}\mathbf{y}$$

$$\{\mathbf{F}_{tp}^e\} = - \int_{h_3}^{h_4} \int_0^{a_e} \int_0^{b_e} [\mathbf{B}_{tb}]^T \{\mathbf{e}_b\} / \mathbf{h}_p \mathbf{d}\mathbf{z}\mathbf{d}\mathbf{x}\mathbf{d}\mathbf{y}$$

and

$$\{\mathbf{F}_{rp}^e\} = - \int_{h_3}^{h_4} \int_0^{a_e} \int_0^{b_e} [\mathbf{B}_{rb}]^T [\mathbf{Z}_b]^T \{\mathbf{e}_b\} / \mathbf{h}_p \mathbf{d}\mathbf{z}\mathbf{d}\mathbf{x}\mathbf{d}\mathbf{y} \quad (14)$$

in which $\mathbf{h}_1 = -h/2$, $\mathbf{h}_4 = h/2 + \mathbf{h}_v + \mathbf{h}_p$, ρ_v and ρ_p are mass densities of the viscoelastic and the 1-3 piezocomposite materials, respectively, and $\{\mathbf{f}\}$ is the externally applied surface traction. Here we have neglected the rotary inertia because of the small thickness of the overall structure. For an element not integrated with the ACLD treatment, the electroelastic coupling matrices become null matrices and the element stiffness matrices are real. Equations (12) and (13) are assembled to obtain the following open loop global equations of motion:

$$[\mathbf{M}] \{\ddot{\mathbf{X}}\} + [\mathbf{K}_{tt}] \{\mathbf{X}\} + [\mathbf{K}_{tr}] \{\mathbf{X}_r\} = \sum_{j=1}^q \{\mathbf{F}_{tp}^j\} \mathbf{V}^j + \{\mathbf{F}\} \quad (15)$$

and

$$[\mathbf{K}_{tr}]^T \{\mathbf{X}\} + [\mathbf{K}_{rr}] \{\mathbf{X}_r\} = \sum_{j=1}^q \{\mathbf{F}_{rp}^j\} \mathbf{V}^j \quad (16)$$

where $[\mathbf{M}]$ is the global mass matrix, $[\mathbf{K}_{tt}]$, $[\mathbf{K}_{tr}]$, and $[\mathbf{K}_{rr}]$ are global stiffness matrices, $\{\mathbf{F}_{tp}\}$, $\{\mathbf{F}_{rp}\}$ are global electroelastic coupling vectors, $\{\mathbf{X}\}$ and $\{\mathbf{X}_r\}$ are global nodal generalized displacement vectors, $\{\mathbf{F}\}$ is the global nodal force vector, q is the number of patches, and \mathbf{V}^j is the voltage difference applied to the j th patch.

Active Damping

The constraining layer of each patch is activated with a voltage proportional to the transverse velocity of a point. That is

$$\mathbf{V}^j = -\mathbf{k}_d^j \dot{\mathbf{w}} = -\mathbf{k}_d^j [\mathbf{U}_t^j] \{\dot{\mathbf{X}}\} - \mathbf{k}_d^j (\mathbf{h}/2) [\mathbf{U}_r^j] \{\dot{\mathbf{X}}_r\} \quad (17)$$

where \mathbf{k}_d^j is the control gain for the j th patch, and unit vectors $[\mathbf{U}_t^j]$ and $[\mathbf{U}_r^j]$ locate the velocity sensors. Substituting from Eq. (17) into Eqs. (15) and (16), equations of motion governing the closed loop dynamics of the overall FG plate/ACLD system become

$$[\mathbf{M}] \{\ddot{\mathbf{X}}\} + \sum_{j=1}^m \mathbf{k}_d^j \{\mathbf{F}_{tp}^j\} [\mathbf{U}_t^j] \{\dot{\mathbf{X}}\} + \sum_{j=1}^m \mathbf{k}_d^j (\mathbf{h}/2) \{\mathbf{F}_{rp}^j\} [\mathbf{U}_r^j] \{\dot{\mathbf{X}}_r\} + [\mathbf{K}_{tt}] \{\mathbf{X}\} + [\mathbf{K}_{tr}] \{\mathbf{X}_r\} = \{\mathbf{F}\} \quad (18)$$

and

$$\sum_{j=1}^m \mathbf{k}_d^j \{\mathbf{F}_{rp}^j\} [\mathbf{U}_r^j] \{\dot{\mathbf{X}}\} + \sum_{j=1}^m \mathbf{k}_d^j (\mathbf{h}/2) \{\mathbf{F}_{tp}^j\} [\mathbf{U}_t^j] \{\dot{\mathbf{X}}_r\} + [\mathbf{K}_{rr}] \{\mathbf{X}_r\} + [\mathbf{K}_{tr}] \{\mathbf{X}\} = 0 \quad (19)$$

Results and Discussion

Using eight noded isoparametric elements, we compute results for square FG Al/Al₂O₃ substrate plates integrated with two ACLD patches, shown in Fig. 1, and the constraining layer composed of the 1-3 PZT-5H/spur composite with 60% volume fraction of PZT-5H fibers. Values assigned to effective material parameters of the piezocomposite are [19] $\mathbf{C}_{11} = 9.29$ GPa, $\mathbf{C}_{12} = 6.18$ GPa, $\mathbf{C}_{13} = \mathbf{C}_{23} = 6.05$ GPa, $\mathbf{C}_{33} = 35.44$ GPa, $\mathbf{C}_{44} = 1.58$ GPa, $\mathbf{C}_{55} = \mathbf{C}_{44}$, $\mathbf{C}_{66} = 1.54$ GPa, $\mathbf{e}_{31} = \mathbf{e}_{32} = -0.1902$ C/m², $\mathbf{e}_{33} = 18.4107$ C/m², and $\rho_p = 5090$ kg/m³. Those for the materials of the FG plate are aluminum: $\mathbf{E}_m = 70$ GPa and $\rho_m = 2707$ kg/m³ and alumina: $\mathbf{E}_c = 380$ GPa and $\rho_c = 3800$ kg/m³; Poisson's ratio for Al and Al₂O₃ is taken to be 0.3. Values of the complex shear modulus, Poisson's ratio, and the mass density of the viscoelastic layer are taken as $20(1+i)$ MPa, 0.49 and 1140 kg/m³, respectively [9]. Unless otherwise mentioned, the thicknesses \mathbf{h} of the FG plate, the viscoelastic layer, and the piezocomposite layer are 0.003 m, 50.8×10^{-6} m and 250×10^{-6} m, respectively, and the length \mathbf{a} of the FG plate equals 0.4 m.

In Table 1 we compare presently computed natural bending frequencies of the simply supported FG plate integrated with the inactive ACLD patches of very small thickness such that their stiffness and mass do not affect the dynamics of the FG plates with those of [28]. It is clear that the two sets of results are in excellent agreement with each other.

To demonstrate the performance of the 1-3 piezocomposite, the frequency response of the ACLD treated FG plate is computed from Eqs. (18) and (19) by exciting it with a time harmonic force of 2 N amplitude applied at the point $(\mathbf{a}/2, \mathbf{a}/4, \mathbf{h}/2)$. The control voltages supplied to the first and the second patches are proportional, respectively, to the transverse velocity of points $(\mathbf{a}/2, \mathbf{a}/4, \mathbf{h}/2)$ and $(\mathbf{a}/2, 3\mathbf{a}/4, \mathbf{h}/2)$. The control gains are chosen to efficiently annul the first few modes. Figure 2 illustrates frequency response functions for the transverse displacement (\mathbf{w}) of the point $(\mathbf{a}/2, \mathbf{b}/4, \mathbf{h}/2)$ for

Table 1 Comparison of natural bending frequencies (ϖ) of square FG plates ($\mathbf{a}/\mathbf{h} = 10$)

FG plates ^a	Source	Mode (1,1)	Mode (1,2)	Mode (2,2)
$\mathbf{n} = 0.5$	Present FEB	0.02517	0.06039	0.09319
	Ref. [28]	0.02521	0.06048	0.09323
$\mathbf{n} = 1.5$	Present FEB	0.02158	0.05178	0.07982
	Ref. [28]	0.02165	0.05188	0.07991

^a $\varpi = \omega \mathbf{h} \sqrt{\rho_0(1+\nu)/\mathbf{E}_0}$, ω is the circular natural frequency, $\rho_0 = 1$ kg/m³, and $\mathbf{E}_0 = 1$ GPa.

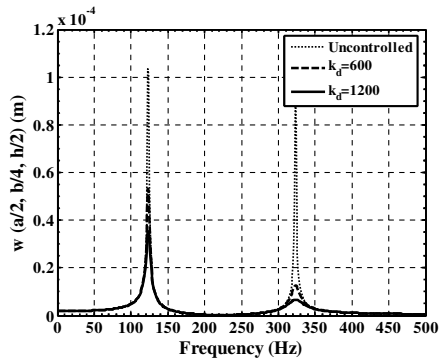


Fig. 2 Frequency response functions for the transverse displacement w of the point $(a/2, a/4, h/2)$ of a simply supported FG plate ($k = 1, n = 2$).

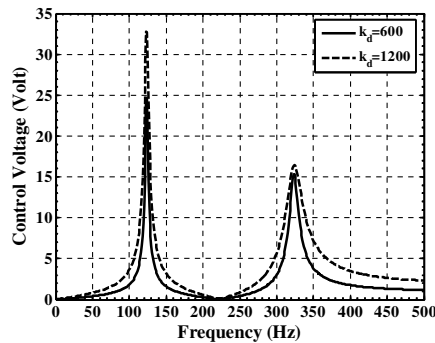


Fig. 3 Variation of the control voltage with the frequency of excitation for the ACLD of the FG plate ($k = 1, n = 2$).

$n = 2$. The variation of the control voltage applied to each patch with the frequency of excitation is shown in Fig. 3. Results plotted in Fig. 2 clearly reveal that if the constraining layer of the ACLD treatment is made of vertically reinforced 1-3 piezocomposite, the activated patches significantly attenuate the amplitude of vibrations, and enhance damping characteristics of the system over that of the passively damped system. Plots of Fig. 3 indicate that the maximum control voltage required to achieve this damping is quite low. To delineate contribution of the vertical actuation in improving the damping characteristics of the FG plate, active control responses of the FG plate for a gain of 1200 are plotted in Fig. 4 with and without considering e_{33} and e_{31} . Note that for $e_{31} = 0$ and $e_{33} \neq 0$, the vertical actuation by the ACLD treatment damps motion of the FG plate. However, when $e_{33} = 0$ and $e_{31} \neq 0$, the in-plane actuation of the ACLD annuls motions of the FG plate. It is evident from results depicted in Fig. 4 that the contribution of the vertical actuation of the ACLD treatment is significantly larger than that of the in-plane

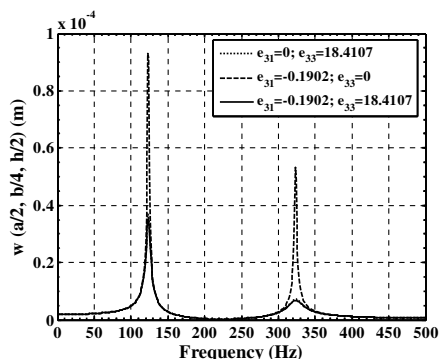


Fig. 4 Frequency response functions for the transverse displacement w of the point $(a/2, a/4, h/2)$ of the FG plate demonstrating the contribution of the transverse actuation of the constraining layer ($k_d = 1200, k = 1, n = 2$).

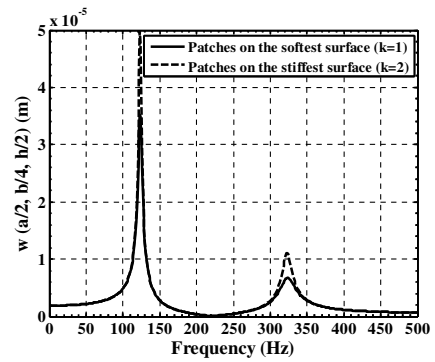


Fig. 5 Comparison of the responses of the FG plate when patches are bonded either to the softest or to the stiffest surface of the plate ($k_d = 1200, n = 2$).

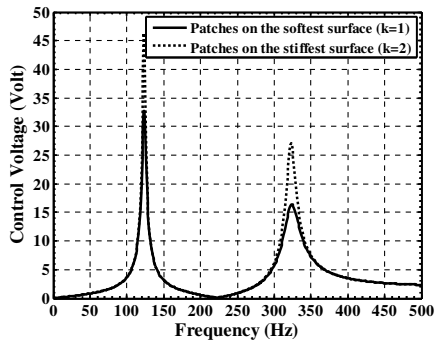


Fig. 6 Comparison of the control voltages for obtaining active responses when patches are bonded either to the softest or to the stiffest surface of the FG plate ($k_d = 1200, n = 2$).

actuation for controlling modes displayed in Fig. 2. This is due to the much higher value of the effective piezoelectric coefficient e_{33} of the 1-3 piezocomposite constraining layer than that of e_{31} . Thus one must consider the transverse normal strain of the constraining layer even if it is a monolithic PZT with $|e_{33}| > |e_{31}|$. It suggests that the shear and normal deformable plate theory of Batra and Vidoli [29] may give better results than the FSDT.

Figures 5 and 6 illustrate that for the same locations ACLD patches bonded to the softest surface (metal rich, $k = 1$) of the FG plate cause more attenuation of vibrations (Fig. 5) with less control voltage (Fig. 6) than when they are attached to the stiffest surface (ceramic rich, $k = 2$) of the plate. Note that in the FG plate material properties vary through the thickness thereby coupling bending and stretching deformations. This coupling is reduced if patches are attached to the softest surface of the substrate FG plate resulting in an improved performance of the ACLD treatment when patches are bonded to the softest surface of the FG plate.

Conclusions

The performance of vertically reinforced 1-3 piezoelectric composite distributed actuator in the ACLD system bonded to a functionally graded FG plate has been investigated. Deformations of each layer in the system are modeled by the first-order shear deformable theory and the resulting 2-dimensional problem is analyzed by the finite element method. The present work considers transverse normal strains induced in each layer thereby using both vertical and in-plane actuations caused by the constraining layer. The frequency response of the FG plate of the system indicates that the active constraining layer of the ACLD treatment significantly enhances damping characteristics of the plate over that caused by passive damping. It is also found that transverse deformations of the constrained layer induce significantly larger damping of the FG plate than that caused by their in-plane deformations. Furthermore, the patches' performance is maximum

when they are bonded to the softest (metal rich) surface of the host FG plate.

References

- [1] Baz, A., and Poh, S., "Performance of an Active Control System with Piezoelectric Actuators," *Journal of Sound and Vibration*, Vol. 126, No. 2, 1988, pp. 327–343.
- [2] Ghosh, K., and Batra, R. C., "Shape Control of Plates Using Piezoceramic Elements," *AIAA Journal*, Vol. 33, No. 7, 1995, pp. 1354–1357.
- [3] Batra, R. C., and Ghosh, K., "Deflection Control During Dynamic Deformations of a Rectangular Plate Using Piezoceramic Elements," *AIAA Journal*, Vol. 33, No. 8, 1995, pp. 1547–1548.
- [4] Batra, R. C., Liang, X. Q., and Yang, J. S., "Shape Control of Vibrating Simply Supported Plates," *AIAA Journal*, Vol. 34, No. 1, 1996, pp. 116–122.
- [5] Batra, R. C., and Liang, X. Q., "Finite Dynamic Deformations of Smart Structures," *Computational Mechanics*, Vol. 20, No. 5, 1996, pp. 427–438.
- [6] Stöbener, U., and Gaul, L., "Modal Vibration Control for PVDF Coated Plates," *Journal of Intelligent Material Systems and Structures*, Vol. 11, No. 4, 2000, pp. 283–293.
- [7] Ray, M. C., "Optimal Control of Laminated Shells with Piezoelectric Sensor and Actuator Layers," *AIAA Journal*, Vol. 41, No. 6, 2003, pp. 1151–1157.
- [8] Lin, J. C., and Nien, M. H., "Adaptive Control of a Composite Cantilever Beam with Piezoelectric Damping-Modal Actuators/Sensors," *Composite Structures*, Vol. 70, No. 2, 2005, pp. 170–176.
- [9] Peng, F., Ng, A., and Hu, Y.-R., "Actuator Placement Optimization and Adaptive Vibration Control of Plate Smart Structures," *Journal of Intelligent Material Systems and Structures*, Vol. 16, No. 3, 2005, pp. 263–271.
- [10] Meng, G., Ye, L., Dong, X. J., and Wei, K. X., "Closed Loop Finite Element Modeling of Piezoelectric Smart Structures," *Shock and Vibration*, Vol. 13, No. 1, 2006, pp. 1–12.
- [11] Baz, A., and Ro, J., "Vibration Control of Plates with Active Constrained Layer Damping," *Smart Materials and Structures*, Vol. 5, No. 3, 1995, pp. 272–280.
- [12] Batra, R. C., and Geng, T. S., "Comparison of Active Constrained Layer Damping by Using Extension and Shear Mode Actuators," *Journal of Intelligent Materials and Structures*, Vol. 13, No. 6, 2002, pp. 249–367.
- [13] Jeung, Y. S., and Shen, I. Y., "Development of Isoparametric, Degenerate Constrained Layer Treatment for Plate and Shell Structures," *AIAA Journal*, Vol. 39, No. 10, 2001, pp. 1997–2005.
- [14] Chantalkhana, C., and Stanway, R., "Active Constrained Layer Damping of Clamped-Clamped Plate Vibrations," *Journal of Sound and Vibration*, Vol. 241, No. 5, 2001, pp. 755–777.
- [15] Ro, J., and Baz, A., "Optimal Placement and Control of Active Constrained Layer Damping Using Modal Strain Energy Approach," *Journal of Vibration and Control*, Vol. 8, No. 6, 2002, pp. 861–876.
- [16] Ray, M. C., and Reddy, J. N., "Optimal Control of Thin Circular Cylindrical Shells Using Active Constrained Layer Damping Treatment," *Smart Materials and Structures*, Vol. 13, No. 1, 2004, pp. 64–72.
- [17] Langote, P. K., and Seshu, P., "Experimental Studies on Active Vibration Control of a Beam Using Hybrid Active/Passive Constrained Layer Damping Treatments," *Journal of Vibration and Acoustics*, Vol. 127, No. 5, 2005, pp. 515–518.
- [18] Piezocomposites, Materials Systems, Inc., 543 Great Road, Littleton, MA 01460.
- [19] Smith, W. A., and Auld, B. A., "Modeling 1–3 Composite Piezoelectrics: Thickness Mode Oscillations," *IEEE Transactions on Ultrasonics, Ferroelectrics and Frequency Control*, Vol. 31, No. 1, 1991, pp. 40–47.
- [20] Hellen, L. C., Kun, Li, and Chung, L. C., "Piezoelectric Ceramic Fiber/Epoxy 1-3 Composite for High Frequency Ultrasonic Transducer Application," *Materials Science and Engineering B*, Vol. 99, No. 1, 2003, pp. 29–35.
- [21] Ray, M. C., and Prodhan, A. K., "The Performance of Vertically Reinforced 1-3 Piezoelectric Composites in Active Damping of Smart Structures," *Smart Materials and Structures*, Vol. 15, No. 2, 2006, pp. 631–641.
- [22] Ootao, Y., and Tanigawa, Y., "Three-Dimensional Transient Thermoelasticity in Functionally Graded Rectangular Plate Bonded to a Piezoelectric Plate," *International Journal of Solids and Structures*, Vol. 37, No. 32, 2000, pp. 4377–4401.
- [23] Wang, B. L., and Noda, N., "Design of a Smart Functionally Graded Thermopiezoelectric Composite Structure," *Smart Materials and Structures*, Vol. 10, No. 2, 2001, pp. 189–193.
- [24] He, X. Q., Ng, T. Y., Sivashanker, S., and Liew, K. M., "Active Control of FGM Plates with Integrated Piezoelectric Sensors and Actuators," *International Journal of Solids and Structures*, Vol. 38, No. 9, 2001, pp. 1641–1655.
- [25] Liew, K. M., He, X. Q., Ng, T. Y., and Kitipornchai, S., "Finite Element Piezothermoelasticity Analysis and the Active Control of FGM Plates with Integrated Piezoelectric Sensors and Actuators," *Computational Mechanics*, Vol. 31, Nos. 3–4, 2003, pp. 350–358.
- [26] Shen, H. S., "Post Buckling of FGM Plates with Piezoelectric Actuators Under Thermo-Electro-Mechanical Loadings," *International Journal of Solids and Structures*, Vol. 42, No. 23, 2005, pp. 6101–6121.
- [27] Ray, M. C., and Sachade, H. M., "Exact Solutions for the Functionally Graded Plates Integrated with a Layer of Piezoelectric Fiber Reinforced Composites," *Journal of Applied Mechanics*, Vol. 73, No. 4, 2006, pp. 622–632.
- [28] Zenkour, A. M., "On Vibration of Functionally Graded Plates According to a Refined Trigonometric Plate Theory," *International Journal of Structural Stability and Dynamics*, Vol. 5, No. 2, 2005, pp. 279–297.
- [29] Batra, R. C., and Vidoli, S., "Higher Order Piezoelectric Plate Theory Derived from a Three Dimensional Variational Principle," *AIAA Journal*, Vol. 40, No. 1, 2002, pp. 91–104.

K. Shivakumar
Associate Editor